

InAs/AlSb Quantum Cascade Detectors Strain-Balanced to GaSb substrates

M. Giparakis¹, S. Isceri¹, W. Schrenk², B. Schwarz¹, G. Strasser¹, and A.M. Andrews¹

1. Institute for Solid-State Electronics, TU Wien, Gußhausstraße 25, 1040 Vienna, Austria
2. Center for Micro- and Nanostructures, TU Wien, Gußhausstraße 25, 1040 Vienna, Austria
aaron.andrews@tuwien.ac.at

Abstract— We present a study on the growth, design, and characterization of strain-compensated InAs/AlSb quantum cascade detectors (QCDs) on GaSb substrates. A QCD detecting at 4.3 μm was designed and grown. HR-XRD and AFM confirm high growth quality and successful strain compensation.

Keywords— quantum cascade detector, InAs/AlSb, GaSb, strain-balancing, mid-infrared, intersubband, photodetector

I. INTRODUCTION

Quantum cascade detectors (QCDs) are mid-infrared photovoltaic detectors built from a heterostructure of alternating well and barrier materials. These devices operate at room temperature and utilize intersubband transitions in the conduction band of the well material [1]. QCDs set themselves apart by high-speed operation enabled by bound-to-bound sub-picosecond intersubband transitions and a designable absorption wavelength [2]. The possible MIR wavelengths depend on the conduction band offset (CBO) of the well and barrier materials and epitaxial growth limitations. These detectors are of interest for applications in chemical spectroscopy [3], imaging [4], and free space optical communication [5]. QCDs were mainly studied for wavelengths $\geq 4 \mu\text{m}$, due to the use of the InGaAs/AlGaAs material system with a CBO of 0.52 eV [6], lattice matched to InP. The InAs/AlSb material system offers the highest CBO in non-polar III-V semiconductors of 2.1 eV [7]. A QCD operating at 2.7 μm was recently realized using InAs/AlAs_{0.16}Sb_{0.84} lattice-matched to an InAs substrate [8]. This QCD needed to be top-side illuminated through a diffraction grating due to the low bandgap of the InAs substrate of 0.35 eV, absorbing below 3.54 μm [6]. On the other hand, InAs offers one of the lowest effective electron masses m_e^* of 0.023 m_0 , which increases the optical transition strength. This is in comparison to InGaAs, which has an effective electron mass m_e^* of 0.043 m_0 . To retain the advantages of the InAs/AlSb material system (high CBO, low m_e^*) and remove the disadvantage of the low InAs bandgap, we present InAs/AlSb-based QCDs grown strain balanced to GaSb substrates.

II. EXPERIMENT AND RESULTS

As a first step, the thermal oxide removal of GaSb and the following GaSb buffer layer was optimized to a root mean square (RMS) surface roughness measured with AFM of 0.273 nm. This was achieved by optimizing the oxide removal

temperature, the temperature during the buffer growth, and the Sb flux for both procedures. In the next step, the growth temperature for the InAs/AlSb heterostructure was optimized. It has to be taken into account that the optimal temperature for InAs differs from AlSb, so an intermediate temperature had to be found for high-quality superlattices. With this, the RMS surface roughness of the InAs/AlSb QCD is 0.286 nm for a $10 \times 10 \mu\text{m}$ area. Figure 1 shows an AFM picture of a $3 \times 3 \mu\text{m}$ scan of the QCD with an RMS surface roughness of 0.189 nm.

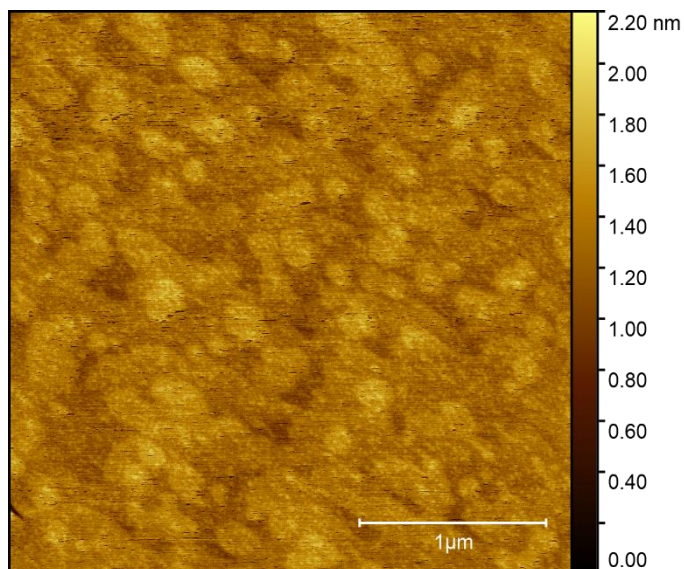


Fig. 1 AFM of a $3 \times 3 \mu\text{m}$ area of the InAs/AlSb QCD grown strain balanced on GaSb. The RMS surface roughness of this scan is 0.189 nm.

Specific shutter sequences and 'soak' times were developed to achieve sharp interfaces between InAs and AlSb and suppress group V intermixing or As-for-Sb exchange, which increases the interface roughness. Additionally, the minimum necessary As and Sb fluxes had to be found. This way, the strain-balancing ratio can be maintained, especially with the thin wells and barriers required for the active region. High-resolution x-ray diffraction (HR-XRD) confirms sharp interfaces and successful strain-balancing, see Fig.2. Strain-compensated growth is necessary, because of the low critical layer thicknesses of InAs

and AlSb on GaSb of ≈ 30 nm. InAs and AlSb strain balance each other with an approximate thickness ratio of 1:1. To achieve high responsivity, InAs and AlSb cannot be kept in the

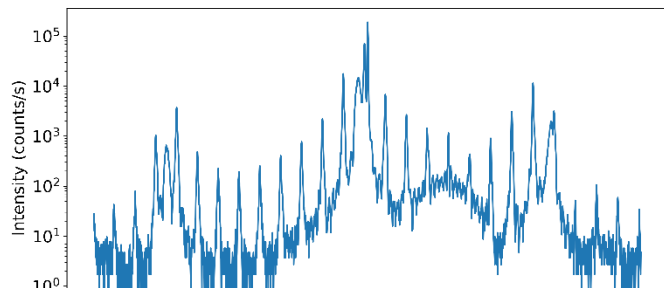


Fig. 2 HR-XRD of an InAs/AlSb QCD grown strain balanced on GaSb with a designed absorption wavelength of $4.3 \mu\text{m}$.

ideal 1:1 ratio for strain balancing, but, for the current design, in a 2.4-to-1 ratio. For this reason, a design technique must be employed, including sub-monolayer-thick InSb layers. Fig.2 showing the HR-XRD of a grown QCD confirms successful strain-balancing with this technique.

The QCD was processed into the 45° wedge-facet substrate illuminated geometry and then optically characterized with a Fourier transform infrared spectrometer (FTIR) and a polarized Globar source. The spectrum shows a QCD absorption at the designed wavelength of $4.3 \mu\text{m}$, and higher energy interband absorptions. Details of the responsivity and the intersubband vs. interband absorption will be discussed.

III. CONCLUSIONS

The high-quality growth of InAs/AlSb heterostructures on GaSb substrates was developed. AFM scans show a low surface roughness of 0.286 nm. HR-XRD confirms high-quality superlattices with sharp peaks. It further confirms successful strain balancing. The QCD was fabricated into the 45° wedge-facet configuration. Optical measurements show an intersubband QCD absorption at the designed wavelength of $4.3 \mu\text{m}$.

ACKNOWLEDGMENTS

The authors acknowledge the financial support from European Office of Aerospace Research and Development/Air Force Office of Scientific Research (FA8655-22-1-7170), Austrian Research Promotion Agency (FFG) Green Sensing Project (Nr. 883941), and the European Research Council (ERC) under the European Union's Horizon 2020 research and innovation program (Grant Agreement Nr. 871529).

REFERENCES

- [1] F. Giorgetta, E. Baumann, M. Graf, Q. Yang, C. Manz, K. Kohler, H. Beere, D. Ritchie, E. Linfield, A. Davies, Y. Fedoryshyn, H. Jackel, M. Fischer, J. Faist, and D. Hofstetter, "Quantum cascade detectors," IEEE J. Quantum Electron. 45, 1039–1052 (2009).
- [2] J Hillbrand, L. M. Krüger, S. Dal Cin, H. Knötig, J. Heidrich, A. M. Andrews, G. Strasser, U. Keller, and B. Schwarz, "High-speed quantum cascade detector characterized with a mid-infrared femtosecond oscillator," Opt. Express 29, 5774-5781 (2021).
- [3] A. Harrer, R. Szedlak, B. Schwarz, H. Moser, T. Zederbauer, D. MacFarland, H. Detz, A. M. Andrews, W. Schrenk, B. Lendl, and G. Strasser, "Mid-infrared surface transmitting and detecting quantum cascade device for gas-sensing," Sci. Rep. 6, 21795 (2016).
- [4] A. Harrer, B. Schwarz, S. Schuler, P. Reininger, A. Wirthmüller, H. Detz, D. MacFarland, T. Zederbauer, A. M. Andrews, M. Rothermund, H. Oppermann, W. Schrenk, and G. Strasser, "4.3 μm quantum cascade detector in pixel configuration," Opt. Express 24, 17041 (2016)
- [5] G. Marschick, M. David, E. Arigliani, N. Opačak, B. Schwarz, M. Giparakis, A. Delga, M. Lagree, T. Poletti, V. Trinite, A. Evirgen, B. Gerard, G. Ramer, R. Maulini, J. Butet, S. Blaser, A. M. Andrews, G. Strasser, and B. Hinkov, "High-responsivity operation of quantum cascade detectors at $9 \mu\text{m}$," Opt. Express 30, 40188-40195 (2022).
- [6] I. Vurgaftman, J. R. Meyer, and L. R. Ram-Mohan, "Band parameters for III–V compound semiconductors and their alloys," J. Appl. Phys. 89, 5815–5875 (2001).
- [7] P. Reininger, T. Zederbauer, B. Schwarz, H. Detz, D. MacFarland, A. M. Andrews, W. Schrenk, and G. Strasser, "InAs/AlAsSb based quantum cascade detector," Appl. Phys. Lett. 107, 081107 (2015).
- [8] M. Giparakis, H. Knötig, H. Detz, M. Beiser, W. Schrenk, B. Schwarz, G. Strasser, and A. M. Andrews, "2.7 μm quantum cascade detector: Above band gap energy intersubband detection", Appl. Phys. Lett. 120, 071104 (2022).